Original Article doi: 10.2176/nmc.oa.2021-0027

Neurol Med Chir (Tokyo) 61, 721–730, 2021 Online October 7, 2021

Intra-arterial Contrast-enhanced Micro-computed Tomography Can Evaluate Intracranial Status in the Ultra-early Phase of Experimental Subarachnoid Hemorrhage in Rats

Ryo MIYAOKA,[1] Junkoh YAMAMOTO,[1] Hiroshi MIYACHI,[1] Kohei SUZUKI,[1] Takeshi SAITO,[1] and Yoshiteru NAKANO[1]

[1]*Department of Neurosurgery, School of Medicine, University of Occupational and Environmental Health, Kitakyushu, Fukuoka, Japan*

Abstract

The endovascular perforation (EP) model is a common technique for experimental subarachnoid hemorrhage (SAH) in rats, simulating the pathophysiological features observed in the acute phase of SAH. Due to the drawbacks of large variations in the amount of bleeding, the results obtained from this model require severity evaluation. However, no less-invasive procedure could confirm the precise intracranial conditions immediately after establishing the rat EP model. We created a novel method for evaluating SAH immediately after establishing the rat EP model using intra-arterial contrast-enhanced micro-computed tomography (CT). We administered contrast agents continuously via the carotid artery during surgery and performed CT examination immediately after SAH induction. First, bleeding severity was classified by establishing a scoring system based on the CT findings (cSAH scoring system). Subsequently, we determined the actual SAH distribution macroscopically and histologically and compared it with the cSAH scores. Second, we investigated the contrast agent's neurotoxicity in rats. Finally, we confirmed the correlation between cSAH scores and SAH severity, including neurological status, cerebral vasospasm, and hematoma volume 24 hr after SAH. Intra-arterial contrast-enhanced micro-CT could visualize the distribution of SAH proportionally to the bleeding severity immediately after establishing the EP model. Moreover, the contrast agent administration was determined not to be neurotoxic to rats. The cSAH scoring revealed a significant correlation with the SAH severity in the rat EP model (P <0.01). Thus, our minimally invasive method provided precise information on intracranial status in the ultra-early phase of SAH in rats EP model.

Keywords: subarachnoid hemorrhage, endovascular perforation, rat model, micro-CT, iodinated contrast agent

Introduction

Aneurysmal subarachnoid hemorrhage (SAH) accounts for approximately 5% of stroke cases, affecting more than 600000 patients annually worldwide. Morbidity among patients with SAH remains high[1–4]; therefore, many researchers have investigated the pathogenesis of SAH to improve its prognosis. To date, animal models of SAH, using several methods, have been established to reproduce the clinical conditions faithfully. These include direct injection of autologous blood into the cisterna magna,[5] transection of a vein in the cistern,[6] or arterial perforation in the circle of Willis using an endovascular filament inserted through the external carotid artery (ECA; endovascular perforation [EP] model).[7–13] Among them, the EP model has been commonly used in basic research on SAH because it mimics the rupture of a cerebral aneurysm and most of its sequelae, such as brain edema formation,[11,14] delayed cerebral

Received January 27, 2021; Accepted August 10, 2021

vasospasm (CVS),[15,16] and neurological dysfunction.[17,18] However, due to the drawbacks of large variations in the amount of bleeding, the results of these experiments require the evaluation of the severity. Some studies have reported measuring intracranial pressure and cerebral blood flow using small catheters inserted into the brain to confirm the induction of SAH indirectly.[1,19] Furthermore, the appearance in isolated brains is commonly used to evaluate SAH severity by sacrificing animals within a few days and then analyzing the experimental data retrospectively in a blinded fashion.[11,18] However, there is no less-invasive procedure that can confirm the intracranial conditions immediately after establishing the rat EP model. Therefore, evaluation of SAH severity in the ultra-early phase is essential in the EP model as like the clinical setting.

Micro-computed tomography (micro-CT) is an effective imaging modality for rodent studies and can clearly visualize the microanatomy of bones and lungs. However, generally, micro-CT cannot visualize the precise microanatomy of the intracranial space compared to that of other organs because of its low-contrast resolution.[20–22]

In this study, we established a novel method for evaluating SAH immediately after the induction of the EP model in rats using intra-arterial contrast-enhanced micro-CT. Here, we discuss the efficacy of our method for assessing the initial intracranial conditions in experimental SAH.

Materials and Methods

Animals

All animal procedures were approved by the Ethics Review Committee for Animal Experimentation of the University of Occupational and Environmental Health, Japan (approval number: AE18-025). A total of 60 adult male Sprague Dawley rats (SLC, Shizuoka, Japan) weighing between 295 and 412 g were used in this study. The animals were anesthetized during surgical and imaging procedures to control motion and minimize distress to the animals.

Micro-CT system

All *in vivo* imaging was performed using a CosmoScan GX (Rigaku Co., Tokyo, Japan). Equipped with X-ray tubes with a focal spot size of 5 μm and a high-resolution two-dimensional flame photometric detector, the scanner allows us to take high-definition CT images with 4.5 μm per pixel and a maximum pixel number of 8000 × 8000 per slice. Scanning was performed immediately after the induction of SAH. The parameters used for the CT scans were as follows: tube voltage, 50 kV; tube current, 160 μA; axial field of view, 45 mm with a spatial resolution of 90 × 90 × 90 μm^3; and an exposure time of 4 min for high-resolution CT acquisitions. In addition, micro-CT scans were performed and voxel values were standardized from the original attenuation values using the air and water portions.

Surgical and imaging procedure

SAH was induced by EP of the internal carotid artery (ICA) bifurcation using the tubing/wire technique, as described in previous studies.[2,19] It was performed with a slight modification that combined the continuous infusion of the contrast agent intra-arterially to channel it in the extravasated blood during SAH induction.

The rats were mechanically ventilated, and anesthesia was maintained by inhalation of 1–3% isoflurane. The ICA was exposed farther from the pterygopalatine artery (PPA) bifurcation while carefully avoiding damage to the hypoglossal nerve. The distal end of the PPA was ligated using a silk suture. The common carotid artery (CCA), ECA, and ICA (distal side to the PPA bifurcation) were temporarily occluded with aneurysm clips, and the distal end of the PPA was severed and retracted to align with the ICA. A hollow polytetrafluoroethylene tube (SUBL-120; Braintree Scientific, Braintree, MA, USA internal diameter: 0.15 mm, outer diameter: 0.30 mm, length: 30 mm) with a tungsten wire (Scientific Instruments Services, Inc., Palmer MA, USA, catalog number W91, diameter: 0.076 mm, length: 31.5 mm) was inserted into the PPA and secured with a silk suture. The ICA and CCA aneurysm clips were removed within 3 min; the distal end of the ECA was ligated. After transecting the ECA, a 24-gauge catheter attached to flexible plastic tubing, connected to a pressure transducer (Living Systems Instrumentation, St Albans City, VT, USA) and a syringe on a mechanical syringe pump (TE-331S; Terumo, Tokyo, Japan), was inserted and secured with two silk sutures, and the ECA aneurysm clip was removed. A continuous intra-arterial infusion of iohexol (Daiichi-Sankyo, Tokyo, Japan), an iodine contrast agent with a concentration of 300 mg/ml, was initiated at a rate of 8 ml/hr (0.13 ml/min). Anesthesia was controlled to maintain a mean arterial pressure of 70–110 mmHg before puncturing. SAH was induced by the tungsten wire inside the tube. Subsequently, the wire and tubing were withdrawn immediately until the tip of the tubing was in line with the stump of the PPA. Continuous infusion of the contrast agent lasted 3 min after puncturing, and images were acquired within 30 min using micro-CT. For the sham group, the surgical procedures were the same except for puncturing the artery.

Study protocol

Visualization of SAH using intra-arterial contrast-enhanced micro-CT in rats EP model

The animals underwent EP surgery with or without a contrast agent, and the intracranial condition was immediately evaluated using micro-CT. Then, the animals were sacrificed immediately under deep anesthesia, and their brains were rapidly removed. For quantitative evaluation of SAH on intra-arterial contrast-enhanced CT findings, we established a novel scoring system based on the CT findings (cSAH scoring system). First, the basal cistern was divided into six segments (right and left ICA terminal portion, right and left ICA–posterior communicating artery bifurcation portion, basilar artery pontine portion, and basilar artery medullary portion). The scoring system was based on the status of contrast enhancement in each segment, which is as follows: grade 0, no enhancement; grade 1, faint enhancement without delineation of the shape of the cistern; grade 2, heterogeneous enhancement with partial delineation of the shape of the cistern; and grade 3, homogenous enhancement with delineation of the full shape of the cistern. Next, the conventional SAH grading system reported by Sugawara et al.[23] was used for the quantitative evaluation of the actual distribution of SAH on macroscopic finding of the brain. Briefly, each segment was assigned a grade from 0 to 3, depending on the amount of subarachnoid blood clotting: grade 0, no subarachnoid blood; grade 1, minimal subarachnoid blood; grade 2, moderate blood clot with recognizable arteries; and grade 3, blood clot obliterating all arteries within the segment. Thus, all animals were rated on a score of 0 to 18 for each system. Finally, scores using the cSAH scoring system were compared with those of the conventional SAH grading system.

In addition, we evaluated the histological findings of these brain specimens based on the CT findings. After image acquisition, the isolated brains were fixed in 10% neutral-buffered formalin (Wako, Tokyo, Japan). The brains were embedded in paraffin and sectioned coronally into 3-mm-thick slices. To evaluate the distribution of SAH and other findings, the brain slices were sub-serially sectioned at 8-μm intervals, deparaffinized, and stained with hematoxylin and eosin (H&E) according to standard protocols.

Evaluation of the neurotoxicity of the contrast agent to rats

Assuming that hemostasis was completed within 1 min at the puncture point in the rat EP model, we calculated 0.13 ml as the maximum amount of contrast agent that flowed into the intracranial space. Thus, a total of 0.1 ml of iohexol (300 mg/ml) was injected into the cisterna magna of rats, as described in a previous study.[1,5,7] The contrast agent was replaced with 0.1 ml physiological saline in the control group.

We compared the body weight and neurological status between the groups at 24 hr and 3, 7, 14, and 38 days. The neurological status was evaluated using a modification of the scoring system reported by Garcia et al.[24] in a blinded fashion. An 18-point scoring system was used to assess sensorimotor deficits, as described in a previous study.[23] This evaluation consisted of six tests: spontaneous activity, symmetrical movements of limbs, forelimb outstretching, wall climbing of a wire cage, axillary touch response, and vibrissae touch response. Each test was assigned a score of 0 or 1–3. The animals were given a score of 3–18 in one-number of steps. Higher scores indicated greater neurological function. The weight gain ratio was calculated by dividing the body weight at each point by that of the control.

Comparison between cSAH scoring system and SAH severity in rats EP model

Immediately after establishing the EP model with a contrast agent, micro-CT imaging was performed as previously described. Twenty-four hours after SAH, the neurological status was evaluated as previously described.

Simultaneously, CVS and SAH hematoma volume were also assessed. These animals underwent perfusion fixation under deep anesthesia 24 hr after SAH, as described in a previous study.[23] Briefly, it was performed by cannulation of the left ventricle and opening of the right atrium. Perfusion was carried out at 60–80 mmHg pressure at room temperature, beginning with 150 mL of 0.1 mol/l PBS (pH 7.4) and followed by 150 ml of 4% paraformaldehyde (Wako, Tokyo, Japan). Then, the brain was immersed in the same fixative at 4°C for 24 hr. A series of samples were used to examine the caliber and morphology of the intracranial arteries. The histological parameters of the ipsilateral ICA were used to assess CVS. Sections of 4-μm thickness were stained with H&E. The diameter (average of major and minor axes), perimeter, and wall thickness were measured in three sequential sections, and the mean value was determined using ImageJ software (US National Institutes of Health, Bethesda, MD, USA).

In addition, hematoma volumes were calculated, as described in a previous study.[25] Briefly, the brains, including the overall length of the circle of Willis and basilar arteries (between −14.6 mm and 2.2 mm from the bregma) were serially sectioned

coronally into 0.4-mm slices. Sections of 4-μm thickness were taken from each slice with a blood clot and stained with H&E. Images of the sections were captured using a digital camera and quantified with ImageJ. The hematoma volume was obtained by multiplying the section thickness with the blood clot area of each slice and summating the hematoma volume of each slice.

Data analysis

Simple regression analysis and Spearman's correlation coefficient by the rank test were performed to assess the correlation between the conventional SAH grade and the cSAH score, the cSAH score, and the neurological score, CVS, or hematoma volume. Student's t-test was performed to assess the neurotoxicity of the contrast agent in rats. Data were expressed as mean ± SEM. Statistical significance was set at $P < 0.05$. A value of $r > 0.4$ was considered a significant correlation, and $r > 0.7$ was considered a strong correlation.

Results

Visualization of SAH using intra-arterial contrast-enhanced micro-CT in rats EP model

Micro-CT could not visualize the distribution of SAH just after establishing the EP model without a contrast agent, despite a large amount of SAH (Fig. 1A). Thus, we tried to evaluate intracranial conditions using micro-CT in a rat EP model with a continuous intra-arterial infusion of the contrast agent. We successfully visualized SAH distribution immediately after establishing the EP model in proportion to the severity of bleeding (Fig. 1B–1E).

Next, we confirmed the correlation between bleeding severity on micro-CT and actual macroscopic bleeding by comparison of the scores of cSAH scoring and conventional SAH grading (Fig. 2A). The cSAH scoring revealed a significant correlation with the conventional SAH grading system immediately after SAH induction ($P = 0.0109$, $r = 0.657$) (Fig. 2B).

Micro-CT clearly showed that the spreading of the contrast agent was not limited to the basal cistern but was extended in the interhemispheric fissure and ventricles. Histological examination showed SAH in the interhemispheric fissure, and intraventricular hemorrhage (IVH) corresponded to the distribution of contrast agents on micro-CT findings (Fig. 3A). Some cases revealed intraparenchymal retention of the contrast agent on micro-CT corresponding to intracerebral hemorrhage (ICH) on histological examination, with large variations. Although the size of ICH was too small to be detected macroscopically, contrast-enhanced micro-CT could clearly depict small ICH as an intraparenchymal high-density lesion (Fig. 3B).

Evaluation of the neurotoxicity of the contrast agent to rats

The weight gain ratio of rats revealed no significant differences between the contrast agent injection group and the control at each point (24 hr, 0.981 ± 0.01 vs 0.984 ± 0.001, $P = 0.67$; day 7, 1.030 ± 0.01 vs 1.047 ± 0.005, $P = 0.16$; day 38, 1.354 ± 0.05 vs 1.354 ± 0.01, $P = 0.99$) (Fig. 4). All animals showed a full score (18/18) as a neurological score at each point; hence, the neurological function showed no significant differences between the groups (data not shown).

Comparison between cSAH scoring system and SAH severity in rats EP model

In this study, the mortality rates were 0% and 42.9% (12 of 28 rats) in the sham and SAH groups, respectively, within 24 hr after SAH induction. All fatal cases showed massive SAH, and the mortality was in agreement with previous reports.[26,27]

To investigate that the cSAH scoring system reflects SAH severity in the rat EP model, we evaluated neurological status, CVS, and hematoma volume, based on the cSAH score (Fig. 5A–5E). We confirmed a strong correlation between the cSAH score and neurological score ($r = -0.941$, $P < 0.01$) (Fig. 5A). ICA diameter and perimeter significantly decreased in inverse proportion to the cSAH score ($r = -0.617$, $P < 0.01$, and $r = -0.695$, $P < 0.01$, respectively) (Fig. 5B and 5C). Conversely, the ICA wall thickness significantly increased in proportion to the cSAH score ($r = 0.842$, $P < 0.01$) (Fig. 5D). Hematoma volume also significantly increased in proportion to the cSAH score ($r = 0.652$, $P < 0.01$) (Fig. 5E).

Discussion

Intra-arterial contrast-enhanced micro-CT can visualize SAH immediately after establishing the rat EP model

Micro-CT could not detect the distribution of SAH in the EP model without using a contrast agent, because of the limitation of contrast resolution for the small intracranial space of rats. Thus, we considered that micro-CT could visualize SAH by enhancing the X-ray absorption of blood using a contrast agent. We developed a novel method to establish a rat EP model using a continuous intra-arterial injection of contrast agent during SAH induction. In particular, micro-CT could visualize the distribution of SAH immediately after establishing the rat EP model. In

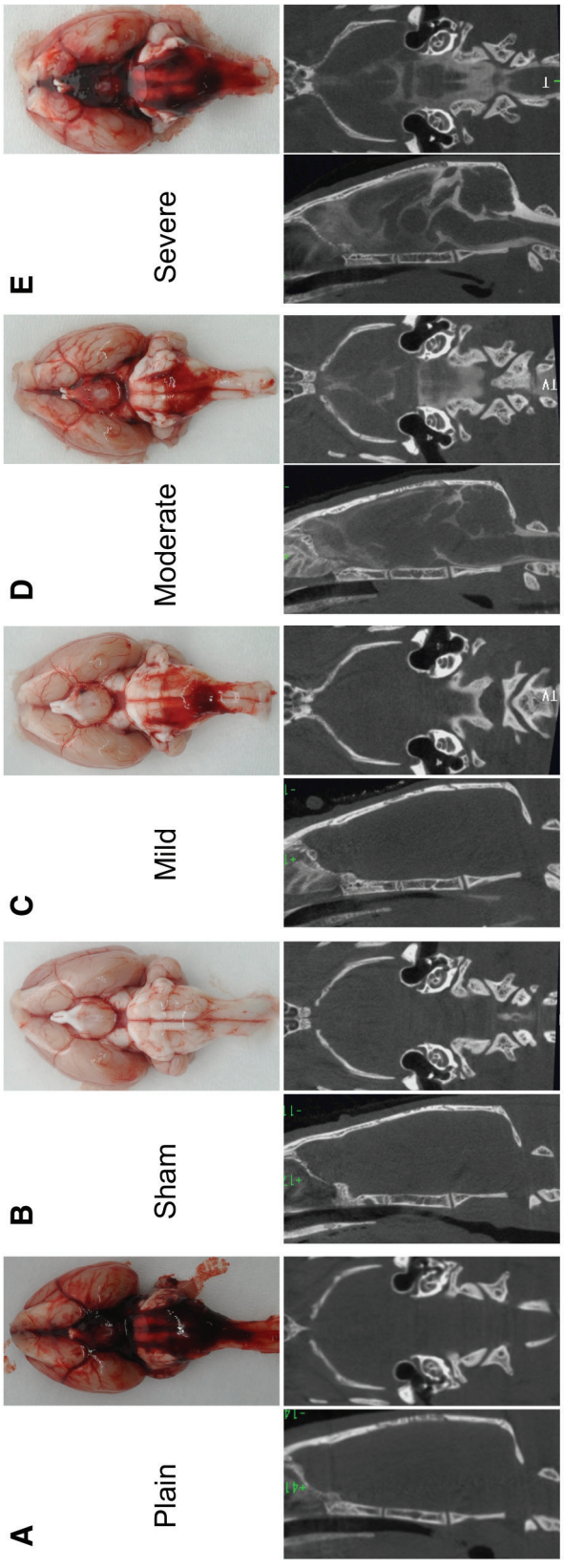

Fig. 1 SAH visualization in an EP rat model by contrast-enhanced micro-CT. The figure shows representative photographs and CT images of (A) plain, (B) sham, (C) mild, (D) moderate, and (E) severe. CT images show sagittal views in the midline (lower left panel) and axial views in the basal cistern (lower right panel). (A) Plain micro-CT cannot visualize the distribution of SAH (n = 3). (C–E) Contrast-enhanced CT images reflect the degree of SAH immediately after induction. (B) The contrast agent does not affect the depiction of any other intracranial structure without extravasation. SAH: subarachnoid hemorrhage, EP: endovascular perforation, CT: computed tomography.

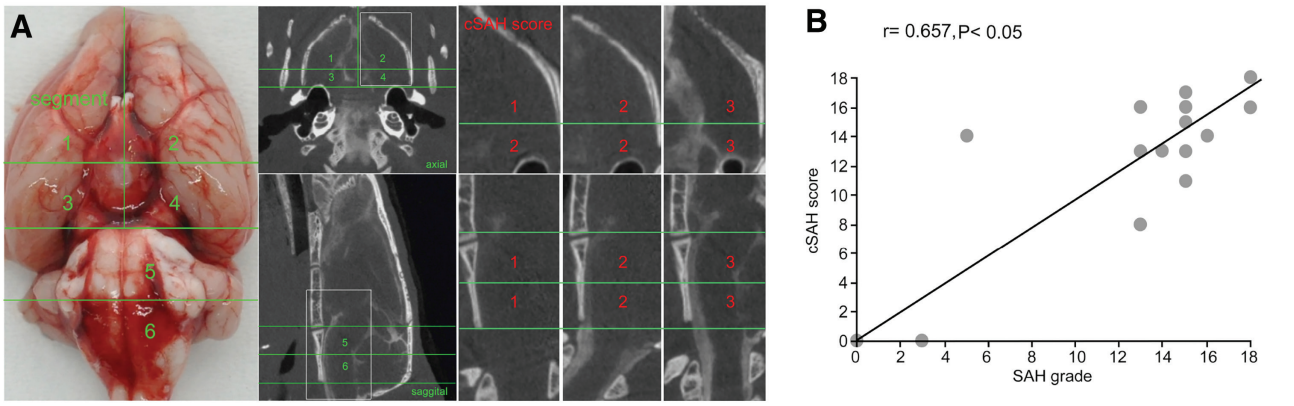

Fig. 2 Correlations between the photographs and CT images depicting the bleeding severity. (A) Division of the basal cistern into six segments in a photograph (left panel) and CT images (right panel). SAH is assessed in each segment to allot a score from 0 to 3, as described previously. The SAH grades are evaluated in photographs, and the cSAH scores are evaluated in axial and sagittal CT images. (B) Relationship between cSAH score and the conventional SAH grade in the rat EP model (n = 16). Data show significant correlation between SAH grade and cSAH score (r = 0.657, P <0.05). CT: computed tomography, SAH: subarachnoid hemorrhage, cSAH score: score for grading SAH based on CT findings, EP: endovascular perforation.

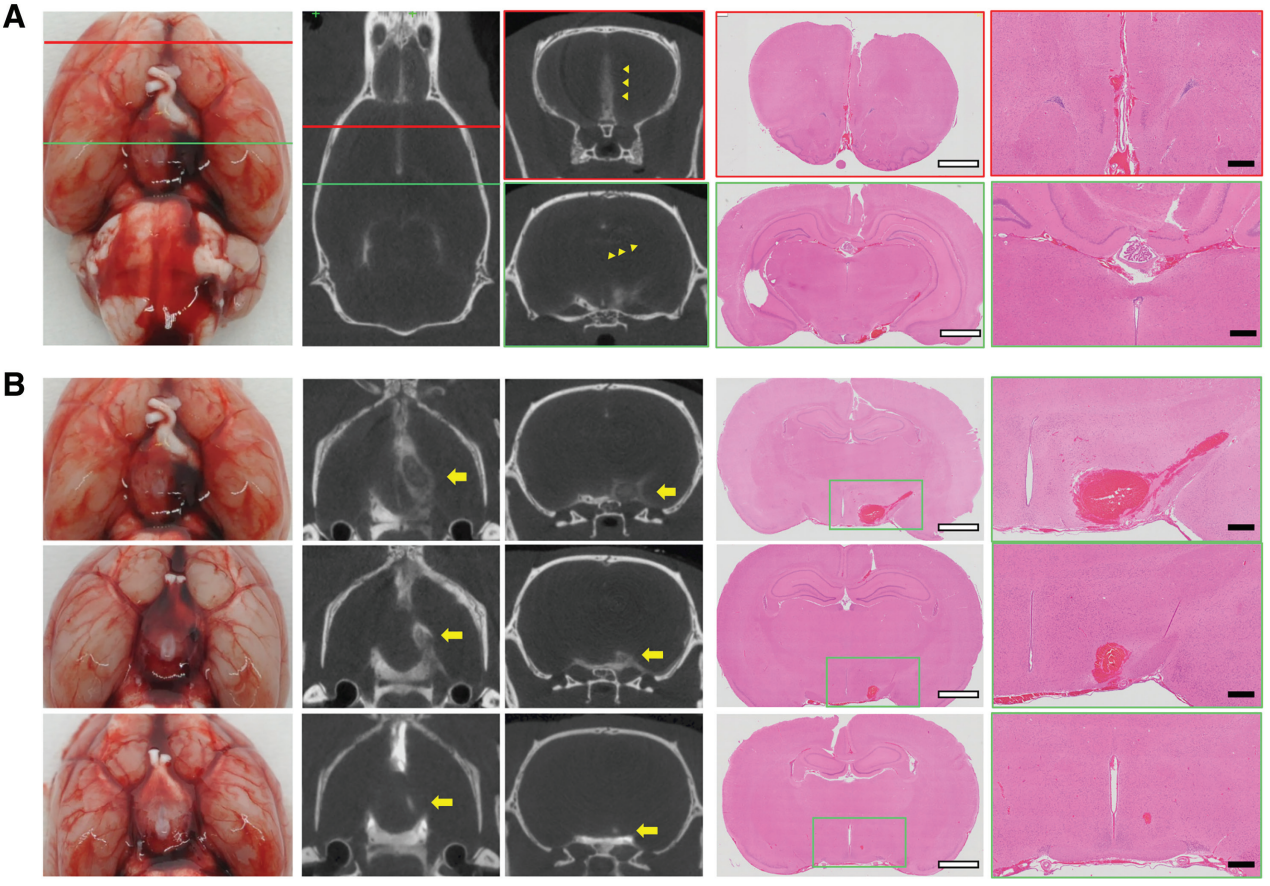

Fig. 3 Comparisons of the intra-arterial contrast-enhanced CT images and pathological findings. (A) CT images depicting the wide distribution of SAH in interhemispheric fissure (red line) and ventricles (green line). Images acquired from the same slice of the SAH brains in CT image and H&E staining. (B) CT images depicting the complication of ICH with large variations (arrow). H&E staining demonstrates ICH formation in the corresponding lesions of the specimen. Scale bars indicate 2 mm (white bars) and 500 μm (black bars), respectively. CT: computed tomography, SAH: subarachnoid hemorrhage, H&E: hematoxylin and eosin, ICH: intracerebral hemorrhage.

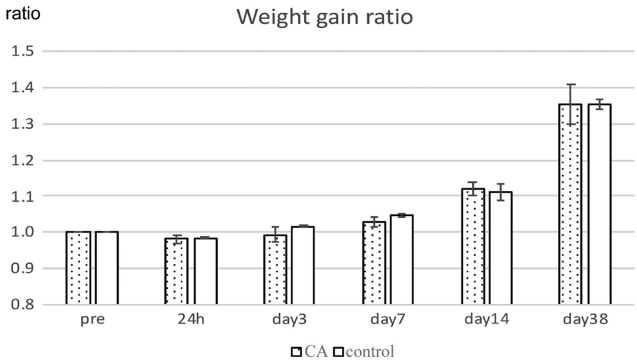

Fig. 4 Weight gain ratio after injection of contrast agent in the cistern of rats. There are no significant differences in weight gain between the contrast agent (n = 4) and physiological saline (*control*, n = 3) groups. Weight gain ratio = pre body weight/post body weight (at 24 hr, 0.981 ± 0.01 vs. 0.984 ± 0.001, P = 0.67; day 7, 1.030 ± 0.01 vs. 1.047 ± 0.005, P = 0.16; day 38, 1.354 ± 0.05 vs. 1.354 ± 0.01, P = 0.99). CA: contrast agent.

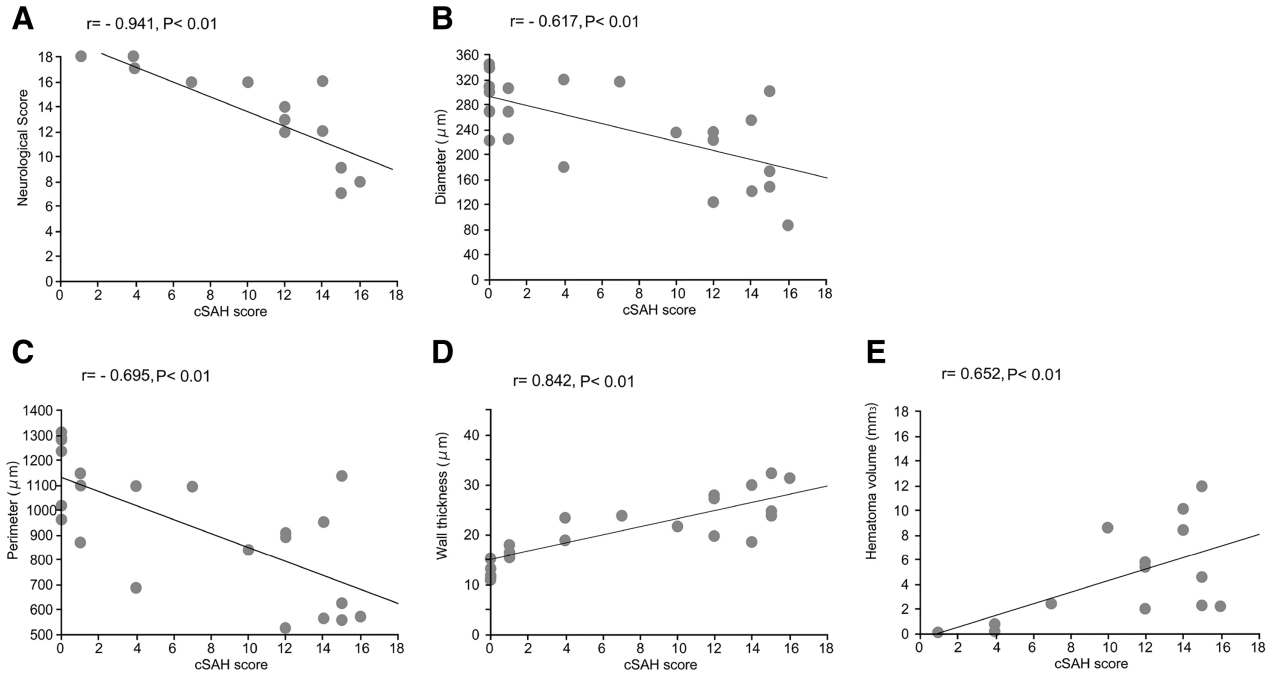

Fig. 5 Correlations of the cSAH score with the neurological score, CVS, and hematoma volume. Animals undergo micro-CT imaging immediately after the establishment of the EP model with a contrast agent. The cSAH score, neurological score, CVS, and hematoma volume are evaluated 24 hr after SAH (n = 16). (A) Neurological score, (B) ipsilateral ICA diameter, (C) ipsilateral ICA perimeter, (D) ipsilateral ICA wall thickness, and (E) hematoma volume. These parameters are significantly correlated with the cSAH score (P <0.01). The three figures of (B–D) also include data from the sham group (n = 6), clustered at grade 0 on the x-axis. CT: computed tomography, EP: endovascular perforation, SAH: subarachnoid hemorrhage, cSAH score: score for grading SAH based on CT findings, CVS: cerebral vasospasm, ICA: internal carotid artery.

addition, we established a novel cSAH scoring system based on the micro-CT findings and confirmed the high detectability of bleeding in this method by comparison of the scores of cSAH scoring and conventional SAH grading.

A few studies on the visualization of SAH in the EP models using imaging modalities have been reported. One study assessed SAH 24 hr after SAH induction using magnetic resonance imaging (MRI).[28] MRI findings of hemorrhage dynamically change based on the oxygenation state of hemoglobin. Generally, the blood in the ultra-early phase of hemorrhage is composed of oxyhemoglobin, which contains a large amount of oxygen, and has a limited

effect on MRI signal intensity. Thus, it is necessary to evaluate SAH using MRI several hours after the induction of the rat EP model. Although it benefits non-invasive procedures, MRI is insufficient to assess the initial intracranial status in a rat EP model.

Meanwhile, a recent study reported a method for determining SAH in the mice EP model using micro-CT with the method for digital subtraction angiography.[22] The authors implanted a vascular access mini port in the jugular vein in advance, induced SAH under the intravenous administration of a large amount (3–5 mg/g body weight) of contrast agent, and then evaluated initial intracranial conditions. However, it may be difficult to distinguish between the cisternal portion of the SAH and surrounding venous systems because the large amount of contrast agent obstructed the visualization of venous structures. Moreover, the high concentration of contrast agent in the arterial phase would take only a few seconds and then decrease rapidly. Thus, it may be difficult to achieve a coincidence of the peak concentration of the contrast agent with the puncturing timing.

In contrast, using our method, we can continuously administer the contrast agent and maintain the intra-arterial high steady concentration at the puncture point during the period from a puncture to hemostasis. In addition, we attenuated the visualization of the venous structure by reducing the administration of the contrast agent. Moreover, intra-arterial contrast-enhanced micro-CT could depict the distribution of SAH to the basal cistern and SAH within the interhemispheric cistern, IVH, and ICH. Thus, our procedure could provide precise information on the intracranial status in the ultra-early phase of SAH in a rat EP model.

Neurotoxicity of the contrast agent is low in rats

Because our procedure needs contrast agent to enhance the X-ray absorption of blood, the neurotoxicity of the contrast agent itself should be excluded in rats. Thus, we used iohexol, which is commonly used as a contrast agent in the myelography of people, in our procedure. We administered the contrast agent intra-arterially, and consequently could reduce the amount (0.6 mg/g body weight). Furthermore, this study confirmed that there was neither body weight loss nor neurological dysfunction using direct cisternal injection of the contrast agent. Therefore, we considered that the influence of the contrast agents contained in extravasated blood for the brain is extremely low in our procedure.

Novel cSAH scoring system can evaluate the SAH severity in the rat EP model

Furthermore, we confirmed that the cSAH scores significantly correlated with the parameters of SAH severity, such as neurological status, CVS, and hematoma volume. Thus, we considered that our procedure could evaluate the SAH severity using the cSAH scoring system in a less-invasive way immediately after establishing the rat EP model.

Recently, many experimental studies have focused on ultra-early changes in the intracranial state of SAH, called early brain injury. These changes have been reported to result in oxidative stress, inflammation, and blood–brain barrier (BBB) disruption, leading to poor prognosis.[18] In clinical situations, aneurysmal SAH complicated with several complex conditions, such as ICH and hydrocephalus, at an early stage, and these phenomena tend to patient prognosis.[29,30] Similarly, these additional phenomena might affect the prognosis of SAH in a rat EP model. Our study demonstrated that micro-CT clearly depicted the various patterns of SAH distribution and minute ICH that could not be detected macroscopically, and IVH, which could cause hydrocephalus, in the ultra-early phase of the rat EP model. Thus, our method would be useful to investigate the relation between the SAH severity with these phenomena and the prognosis in the EP model.

Limitations

We could not exclude the biological effect of intra-arterial administration of the contrast agent on the pathological condition after SAH completely. Further studies may be required to determine the long-term pathophysiological effects of this method.

Conclusion

We developed a novel method for visualizing hemorrhagic changes immediately after SAH induction using micro-CT with a continuous intra-arterial infusion of a contrast agent in a rat EP model. Our method could provide more precise information about intracranial status in the ultra-early phase in a rat EP model, allowed us to evaluate SAH severity prior to intervention, and provided opportunities for long-term observation.

Acknowledgments

We thank Takumi Sozen for contributing to the discussion of the manuscript, and Yu Hasegawa and

Yushin Takemoto for providing guidance through the methods.

Funding

This study was supported by Grant-in-Aid for Early-Career Scientists (No. 19K16301) from the Japan Society for the Promotion of Science. The funders had no role in the study design, data collection, analysis, decision to publish, or manuscript preparation.

Conflicts of Interest Disclosure

None.

References

1) Kamp MA, Dibué M, Sommer C, Steiger HJ, Schneider T, Hänggi D: Evaluation of a murine single-blood-injection SAH model. *PLoS One* 9: e114946, 2014
2) Bühler D, Schüller K, Plesnila N: Protocol for the induction of subarachnoid hemorrhage in mice by perforation of the Circle of Willis with an endovascular filament. *Transl Stroke Res* 5: 653–659, 2014
3) Feigin VL, Lawes CM, Bennett DA, Barker-Collo SL, Parag V: Worldwide stroke incidence and early case fatality reported in 56 population-based studies: a systematic review. *Lancet Neurol* 8: 355–369, 2009
4) King JT: Epidemiology of aneurysmal subarachnoid hemorrhage. *Neuroimaging Clin N Am* 7: 659–668, 1997
5) Lin CL, Calisaneller T, Ukita N, Dumont AS, Kassell NF, Lee KS: A murine model of subarachnoid hemorrhage-induced cerebral vasospasm. *J Neurosci Methods* 123: 89–97, 2003
6) Altay T, Smithason S, Volokh N, Rasmussen PA, Ransohoff RM, Provencio JJ: A novel method for subarachnoid hemorrhage to induce vasospasm in mice. *J Neurosci Methods* 183: 136–140, 2009
7) Fanizzi C, Sauerbeck AD, Gangolli M, Zipfel GJ, Brody DL, Kummer TT: Minimal long-term neurobehavioral impairments after endovascular perforation subarachnoid hemorrhage in mice. *Sci Rep* 7: 7569, 2017
8) Hasegawa Y, Suzuki H, Altay O, Zhang JH: Preservation of tropomyosin-related kinase B (TrkB) signaling by sodium orthovanadate attenuates early brain injury after subarachnoid hemorrhage in rats. *Stroke* 42: 477–483, 2011
9) Milner E, Holtzman JC, Friess S, et al.: Endovascular perforation subarachnoid hemorrhage fails to cause Morris water maze deficits in the mouse. *J Cereb Blood Flow Metab* 34: 1571–1572, 2014
10) Sherchan P, Lekic T, Suzuki H, et al.: Minocycline improves functional outcomes, memory deficits, and histopathology after endovascular perforation-induced subarachnoid hemorrhage in rats. *J Neurotrauma* 28: 2503–2512, 2011
11) Sozen T, Tsuchiyama R, Hasegawa Y, et al.: Role of interleukin-1beta in early brain injury after subarachnoid hemorrhage in mice. *Stroke* 40: 2519–2525, 2009
12) Sun CM, Enkhjargal B, Reis C, et al.: Osteopontin attenuates early brain injury through regulating autophagy-apoptosis interaction after subarachnoid hemorrhage in rats. *CNS Neurosci Ther* 25: 1162–1172, 2019
13) Suzuki H, Hasegawa Y, Chen W, Kanamaru K, Zhang JH: Recombinant osteopontin in cerebral vasospasm after subarachnoid hemorrhage. *Ann Neurol* 68: 650–660, 2010
14) Liu S, Tang J, Ostrowski RP, Titova E, et al.: Oxidative stress after subarachnoid hemorrhage in gp91phox knockout mice. *Can J Neurol Sci* 34: 356–361, 2007
15) Kamii H, Kato I, Kinouchi H, et al.: Amelioration of vasospasm after subarachnoid hemorrhage in transgenic mice overexpressing CuZn-superoxide dismutase. *Stroke* 30: 867–871, discussion 872, 1999
16) Saito A, Kamii H, Kato I, et al.: Transgenic CuZn-superoxide dismutase inhibits NO synthase induction in experimental subarachnoid hemorrhage. *Stroke* 32: 1652–1657, 2001
17) Gao J, Wang H, Sheng H, et al.: A novel apoE-derived therapeutic reduces vasospasm and improves outcome in a murine model of subarachnoid hemorrhage. *Neurocrit Care* 4: 25–31, 2006
18) Uekawa K, Hasegawa Y, Ma M, et al.: Rosuvastatin ameliorates early brain injury after subarachnoid hemorrhage via suppression of superoxide formation and nuclear factor-kappa B activation in rats. *J Stroke Cerebrovasc Dis* 23: 1429–1439, 2014
19) Park IS, Meno JR, Witt CE, et al.: Subarachnoid hemorrhage model in the rat: modification of the endovascular filament model. *J Neurosci Methods* 172: 195–200, 2008
20) Seo Y, Hashimoto T, Nuki Y, Hasegawa BH: In vivo microCT imaging of rodent cerebral vasculature. *Phys Med Biol* 53: N99–107, 2008
21) Hayasaka N, Nagai N, Kawao N, et al.: In vivo diagnostic imaging using micro-CT: sequential and comparative evaluation of rodent models for hepatic/brain ischemia and stroke. *PLoS One* 7: e32342, 2012
22) Weyer V, Maros ME, Kronfeld A, et al.: Longitudinal imaging and evaluation of SAH-associated cerebral large artery vasospasm in mice using micro-CT and angiography. *J Cereb Blood Flow Metab* 40: 2265–2277, 2020
23) Sugawara T, Ayer R, Jadhav V, Zhang JH: A new grading system evaluating bleeding scale in filament perforation subarachnoid hemorrhage rat model. *J Neurosci Methods* 167: 327–334, 2008
24) Garcia JH, Wagner S, Liu KF, Hu XJ: Neurological deficit and extent of neuronal necrosis attributable to middle cerebral artery occlusion in rats. *Statistical validation. Stroke* 26: 627–634, discussion 635, 1995

25) Liew HK, Cheng HY, Huang LC, et al.: Acute alcohol intoxication aggravates brain injury caused by intracerebral hemorrhage in rats. *J Stroke Cerebrovasc Dis* 25: 15–25, 2016
26) Lee JY, Sagher O, Keep R, Hua Y, Xi G: Comparison of experimental rat models of early brain injury after subarachnoid hemorrhage. *Neurosurgery* 65: 331–343, discussion 343, 2009
27) Takemoto Y, Hasegawa Y, Hayashi K, et al.: The stabilization of central sympathetic nerve activation by renal denervation prevents cerebral vasospasm after subarachnoid hemorrhage in rats. *Transl Stroke Res* 11: 528–540, 2020
28) Shishido H, Egashira Y, Okubo S, et al.: A magnetic resonance imaging grading system for subarachnoid hemorrhage severity in a rat model. *J Neurosci Methods* 243: 115–119, 2015
29) Schütz H, Krack P, Buchinger B, et al.: Outcome of patients with aneurysmal and presumed aneurysmal bleeding. A hospital study based on 100 consecutive cases in a neurological clinic. *Neurosurg Rev* 16: 15–25, 1993
30) Broderick JP, Brott TG, Duldner JE, Tomsick T, Leach A: Initial and recurrent bleeding are the major causes of death following subarachnoid hemorrhage. *Stroke* 25: 1342–1347, 1994

Corresponding author: Ryo Miyaoka, MD
Department of Neurosurgery, School of Medicine, University of Occupational and Environmental Health, 1-1 Iseigaoka, Yahatanishi-ku, Kitakyushu, Fukuoka 807-8555, Japan.
e-mail: 38spec@med.uoeh-u.ac.jp